Article

Evaluation of Rheological and Lubrication Properties of Selected Alcohol Fuels

Leszek Chybowski [1] **, Wojciech Wójcik** [2] **and Marcin Szczepanek** [3,*]

1   Department of Marine Propulsion Plants Operation, Faculty of Marine Engineering, Maritime University of Szczecin, ul. Willowa 2, 71-650 Szczecin, Poland; l.chybowski@pm.szczecin.pl
2   Laboratory of Marine Propulsion Plants, Faculty of Marine Engineering, Maritime University of Szczecin, ul. Wały Chrobrego 1-2, 70-500 Szczecin, Poland; wojciech.wojcik@pm.szczecin.pl
3   Department of Power Engineering, Faculty of Marine Engineering, Maritime University of Szczecin, ul. Willowa 2, 71-650 Szczecin, Poland
*   Correspondence: m.szczepanek@pm.szczecin.pl; Tel.: +48-91-4809376

Abstract: This article presents the results of a study on the rheological and lubricating properties of selected alcohol fuels. Methanol, ethanol, and 2-propanol are investigated, for which density, kinematic, and dynamic viscosity are determined at selected temperatures in the range of 15–60 °C. In addition, the water content of the studied fuels is determined. Based on the measurements, the coefficient of temperature change for density and the relative percentage decrease in kinematic viscosity with increasing temperature are calculated. Subsequently, regression models are built to describe the value of density and viscosity of the tested liquid alcohol fuels as a function of temperature. Next, the fuels under study are subjected to the evaluation of antiwear properties using a high-frequency reciprocating rig (HFRR). For each fuel, the corrected wear scar size $WS_{1.4}$, which is a measure of lubricity, the average coefficient of friction, and the relative percentage decrease in oil *FILM* thickness during the conduct of the HFRR test under standardized conditions, are determined. The measurements are carried out at a standardized temperature of 25 °C in accordance with standardized methods for a time equal to 75 min. Due to the low lubricity of the tested fuels, additional tests are performed at a reduced time equal to 30 min. In this case, all fuels show a similar $WS_{1.4}$ value, which ranges from 384 μm for methanol through 422 μm for 2-propanol to 426 μm for ethanol. The wear marks on the samples after the execution of the test are used to draw additional qualitative conclusions about the lubricating properties of the tested alcohols. The results obtained are summarized, and possibilities for their use in further research are provided.

Keywords: alcohol fuel; methanol; ethanol; 2-propanol; lubricity; viscosity; density; HFRR test; high-frequency reciprocating rig; tribological wear

1. Introduction

In recent years, growing interest has arisen in using alcohol fuels to power internal combustion engines as an alternative to fossil fuels. The use of alcohol as fuel in engines has been known for more than a century [1,2]. Today, due to the implementation of climate agreements, including "Fit for 55", the use of alcohols as gasoline admixtures [3] and stand-alone fuels [4] is growing. This is especially true for low-carbon fuels and the use of bio-based fuels such as biomass or biofuels [5].

Due to the phase-out of lead in all grades of gasoline and the adverse health and environmental impacts of tert-butyl methyl ether (MTBE), the synthesis of higher alcohols,

particularly ethanol, from syngas has attracted considerable interest. Low molecular weight alcohols such as ethanol have replaced other admixtures as octane enhancers in automotive fuels. Adding alcohols to petroleum products allows the fuel to burn more completely in the presence of oxygen, which increases combustion efficiency and reduces air pollution. To best utilize alcohols as alternative fuels, the engine or vehicle can be redesigned, or one or more admixtures can be added to ethanol or methanol to improve its properties [6]. Alternative fuels such as alcohols are widely used as admixtures in CI engines. Alcohols have economic advantages in diesel engines compared to conventional diesel fuel and can be used as an additive in compression ignition engines without any engine modifications [7]. Methanol fuel (CH_3OH) is considered one of the optimal fuels for internal combustion engines [8,9]. In addition, ethanol (C_2H_5OH) is considered as one of the most important components of biodiesel fuel and a promising alternative fuel in combustion engines [10–13]. On the other hand, the use of the studied alcohols as promising stand-alone fuels for industrial and marine internal combustion engines is driven by their low cetane number and high octane number, making them excellent fuels for spark-ignition engines. At the same time, these fuels exhibit low autoignition propensity, which significantly limits their application in compression-ignition engines.

A potential solution to these challenges is the use of dual-fuel engines powered by alcohol, where the ignition of the alcohol-air mixture is initiated by the autoignition of a pilot dose of diesel-type fuel. These solutions are currently being intensively developed by leading global manufacturers of large and high-power internal combustion engines, including MAN, Wärtsilä, and WinGD. The technological advancements pursued by these manufacturers mainly focus on methanol, as it is the low-carbon fuel with the fewest carbon atoms per molecule. Such engines are already commercially available and essentially represent the only alternative to low-carbon fuels such as LNG/CNG, LPG, or ethylene.

All the fuels mentioned in the previous sentence can be considered transitional fuels; however, the market will ultimately shift its focus toward carbon-free and low-carbon fuels. Carbon-free fuels such as hydrogen and ammonia still pose significant challenges related to proper storage, corrosive effects, and low volumetric energy density. Among low-carbon fuels, methanol appears to be the most promising option, and it is analyzed in our publication alongside two other low-carbon fuels. All the fuels examined in this article present significant challenges concerning their impact on engine component wear. They were selected and studied within this context. Currently, ethanol and methanol attract attention mainly due to their presence in the market and their potential to improve safety and reduce the negative impact of climate change. Methanol and ethanol are considered as promising oxygen admixtures in reducing CO and NO_x emissions [14,15]. In addition, many esters processed from methanol and ethanol have been used as admixtures blended with diesel fuel in diesel engines [16–20]. Methanol and ethanol are among the most promising alternative sources in terms of low emissions and low costs to replace conventional fuels. They are produced mainly from renewable sources, which makes them more valuable and makes it easier to meet demand in the event of overconsumption.

Aliphatic alcohols with the shortest hydrocarbon chains with one hydroxyl group are methanol, ethanol, and propanol. Propanol exists in the form of two isomers: 1- and 2-propanol. The basic characteristics of methanol, ethanol, and 2-propanol (isopropanol, propan-2-ol), i.e., alcohols used as the fuel in this study, are summarized based on various sources in Table 1.

Table 1. Physicochemical properties of the analyzed alcohol fuels [3,21–23].

Parameter	Fuel		
	Methanol	**Ethanol**	**2-Propanol**
Density at 20 °C (g/cm^3)	0.791–0.792	0.805–0.812	0.784–0.787
Kinematic viscosity at 20 °C (mm^2/s)	0.757	1.333	2.826
Dynamic viscosity at 20 °C (mPa·s)	0.599	1.078	2.220
Molar mass (g/mol)	32.040	46.068	60.110
Calorific value at 15.5 °C (MJ/kg)	19.90	26.80	31.00
Lower explosive limit in air at atmospheric pressure (% vol.)	5.5	3.3	2.0
Upper explosive limit in air at atmospheric pressure (% vol.)	50	19	13
Excess air factor (-)	6.40	9.00	~10.33
Boiling point at atmospheric pressure (°C)	64–65	78–79	81–83
Flash point (in a closed crucible) (°C)	11–12.0	12–18.3	11.7–15
Autoignition temperature (°C)	455–470	373–425	350–425
Octane number (research) RON (-)	108.7	107.4	112.5
Cetane number CN (-)	5	5–15	~12

Alcohols have a low cetane number (low self-ignition tendency), so they are unsuitable as a stand-alone fuel for compression-ignition engines [24]. However, they are used together with pilot liquid hydrocarbon fuel in dual-fuel compression-ignition engines [25], and due to their high octane number, they can be used in spark-ignition engines [26]. Recently, methanol has attained the most popularity as a carbon fuel containing only one carbon atom [27].

One significant challenge of using alcohols as fuel is their lubricity and corrosive effects [28,29], which can result in accelerated wear and damage to machinery powered by such fuel [30]. This also applies to other alcohols used as a stand-alone fuel [31]. In the case of internal combustion engines, the use of alcohol fuels, among others, is considered in the context of their components in blends with diesel oils [32], blends with gasoline [33], or the use of these fuels alone after appropriate treatment with admixtures that improve lubricity [34,35].

Despite a very rich literature describing studies of blending fuels of different types and various aspects of the use of alcohol fuels, the authors did not find any cross-discipline articles that compile the basic rheological and tribological properties of the simplest aliphatic alcohols, which is the motivation for conducting the experiment, that are summarized in this article.

Further research will focus on improving the lubrication properties and reducing corrosion caused by alcohol fuels, which will allow their wider use in combustion engines, and on optimizing fuel mixtures to increase combustion efficiency and reduce harmful emissions.

2. Materials and Methods

The employed experiment used certified alcohol fuels: methanol p.a. 99.85% (PTH CHEMLAND Zbigniew Bartczak, Stargard, Poland), ethanol p.a. 96.00% (Honeywell Specialty Chemicals Seelze GmbH, Seelze, Germany), and 2-propanol p.a. 99.80% (PTH CHEMLAND Zbigniew Bartczak, Stargard, Poland).

In order to holistically assess the effect of the tested fuels on the wear of engine components (i.e., precision injector pairs, fuel pumps, and valves) that can seize, selected rheological and tribological parameters were measured. The procedure adopted in the

experiment is shown in Figure 1. A summary of the measurement data is provided in Appendix A.
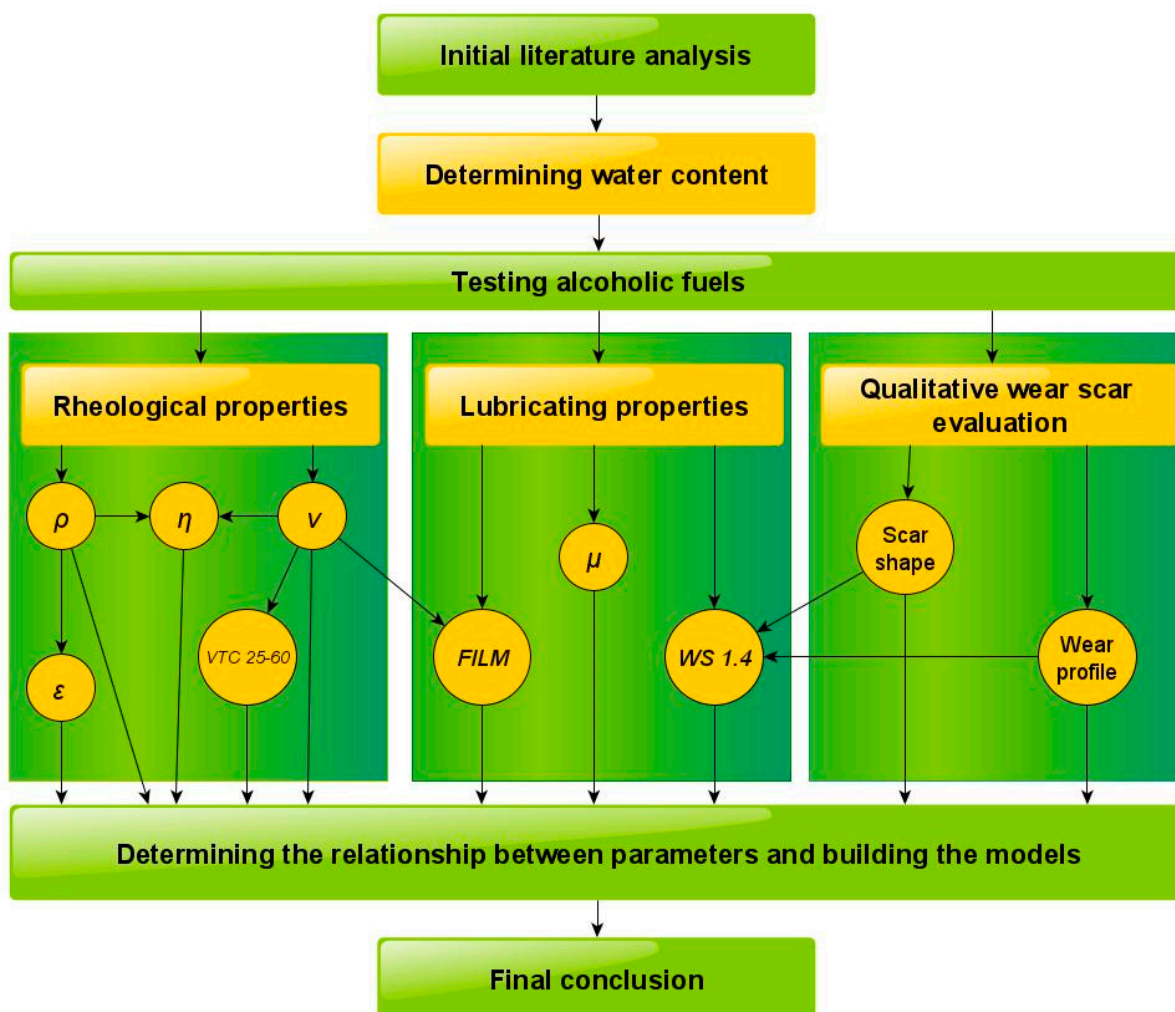

Figure 1. Scheme adopted for the experiment.

Considering the hygroscopic nature of alcohols, the water content was measured for each fuel to best describe the material used in the experiment. This water content testing was determined using the Karl–Fischer method with an 831 KF Coulometer (Metrohm, Herisau, Switzerland). The measured water content in the tested fuels is presented in Table 2.

Table 2. Measured water content of the tested fuels.

Parameter	Fuel		
	Methanol	**Ethanol**	**2-Propanol**
Water content (% m/m)	0.02	5.50	0.13

The rheological properties of alcohols were described using viscosity. Based on the measured values of kinematic viscosity and density, the dynamic viscosity was calculated. The reference density measurement of the petroleum products is usually taken at 15 °C [36]. The viscosity of petroleum-based fuels and lubricating oils is usually determined at 40 °C and 100 °C [37].

In the present experiment, the density of each fuel was determined at 15 °C, 25 °C, 40 °C, and 60 °C, while the kinematic and dynamic viscosities were determined at 25 °C, 40 °C, and 60 °C. The lower value is limited by the capabilities of the measuring apparatus, while the upper value relates to the proximity to the boiling point for one of the fuels tested, i.e., methanol, which is 64–65 °C. Each measurement of the density and kinematic viscosity was made twice, and the value that is recorded is the average of the two measurements. Dynamic viscosity was calculated based on the measured density and kinematic viscosity. Information about the instruments used and the standards according to which the measurements were made, as well as the accuracy of the measurements, is summarized in Table 3.

Table 3. Information on the apparatus and methods used to determine the rheological parameters of the alcohol fuels under study.

Parameter	Apparatus Used	Standard of Measurement Implementation	Accuracy of Measurement	Accuracy of the Temperature Setting
Density	DMA 4500 density analyzer with an oscillating U-tube (Anton Paar GmbH, Graz, Austria)	ISO 12185: 2024 [36]	5×10^{-5} g/cm^3	0.02 °C
Kinematic viscosity	Cannon-Fenske Opaque glass capillary viscometer (Paradise Scientific Company Ltd., Dhaka, Bangladesh) and a TV 2000 viscometric bath (Labovisco bv, Zoetermeer, The Netherlands)	ISO 3104:2023 [37]	0.1%	0.01 °C

In the next step, the variation of density and kinematic viscosity as a function of temperature was evaluated. For this purpose, the coefficient of temperature change in density and the relative percentage decrease in kinematic viscosity with increasing temperature were found. Regression models were also built to describe the variation of density, kinematic viscosity, and dynamic viscosity as a function of temperature. For each model, the quality of the model fit to the experimental data was evaluated using the coefficient of determination. A summary of the developed models is provided in Appendix B.

The tribological properties of the tested fuels were determined using the high-frequency reciprocating rig (HFRR) from which the corrected wear scar $WS_{1.4}$ (lubricity [38]) was found, as well as the average coefficient of friction and the relative percentage decrease in oil *FILM* thickness during the execution of the HFRR test. Considering the high wear intensity of the samples separated by a layer of test fuels, the measurements were performed at a test execution temperature of 25 °C in accordance with ISO 12156:2023 [39], ASTM D6079-22 [40]. The ASTM D6079 standard is essentially identical in content to the other two standards, CEC F-06-96 [41] and ISO 12156:2023. The difference concerns the testing of low-lubricity fuels, where only the ASTM D6079 standard allows for lubricity testing at temperatures lower than 60 °C. Moreover, CEC F-06-96 is now obsolete [42]. It should be noted that the HFRR apparatus used meets the measurement requirements in accordance with both ASTM D6079 and ISO 12156:2023 standards. The lubricity tests were carried out at a standard time τ of 75 min and a shortened test execution time τ of 30 min. In addition to the quantitative evaluation of lubricity and auxiliary indicators, a qualitative assessment was made on the wear scar produced during each HFRR test. Infor-

mation on the apparatuses used, and the standards according to which the measurements of tribological parameters were carried out are summarized in Table 4.

Table 4. Information about the apparatuses and methods used to determine the tribological parameters of the alcohol fuels under study.

Parameter	Apparatus Used	Standard of Measurement Implementation	Accuracy of Measurement	Accuracy of the Temperature Setting
Lubricity	HFRR V1.0.3 tribometer [43] and HFRR microscope [44] (PCS Instruments, London, UK)	ASTM D6079-22 [40]	50 μm	80 μm
Average coefficient of friction	Cannon-Fenske Opaque glass capillary viscometer (Paradise Scientific Company Ltd., Dhaka, Bangladesh) and a TV 2000 viscometric bath (Labovisco bv, Zoetermeer, The Netherlands)	HFRR V.1.0.3 procedure [43]	Auxiliary parameter Not applicable	Auxiliary parameter Not applicable
Percentage decrease in oil *FILM* thickness		HFRR V.1.0.3 procedure [43]	Auxiliary parameter Not applicable	Auxiliary parameter Not applicable

In view of the fact that lubricity is not a fundamental physical quantity, its measurement accuracy is not specified. Instead, the standards include information on the repeatability and reproducibility of the measurements, which are determined based on statistical analyses of results obtained in different laboratories for a given set of samples.

3. Results and Discussion

3.1. Rheological Indices

The density of the alcohol fuels tested as a function of their temperature is shown in Figure 2. The dotted lines show the curves approximating each set of measurements. Ethanol has the highest density, and 2-propanol has the lowest.

The density ρ_t (kg/m^3) of each of the studied alcohols, likewise for fossil fuels, decreases approximately linearly with increasing temperature and can be determined at a given temperature t (°C) relative to the reference density ρ_{15} (kg/m^3) of a given liquid at 15 °C according to a relationship commonly used in engineering applications, which is described by the following formula [45]:

$$\rho_t = \rho_{15} - \varepsilon(t - 15),\tag{1}$$

where ε (kg/(m^3·°C)) is the coefficient of temperature change for liquid density.

For the tested alcohols and the temperature difference between 15 °C and 60 °C, the coefficient ε can be calculated using the densities at the relevant temperatures, i.e., ρ_{15} (kg/m^3) and ρ_{60} (kg/m^3), according to the following relationship:

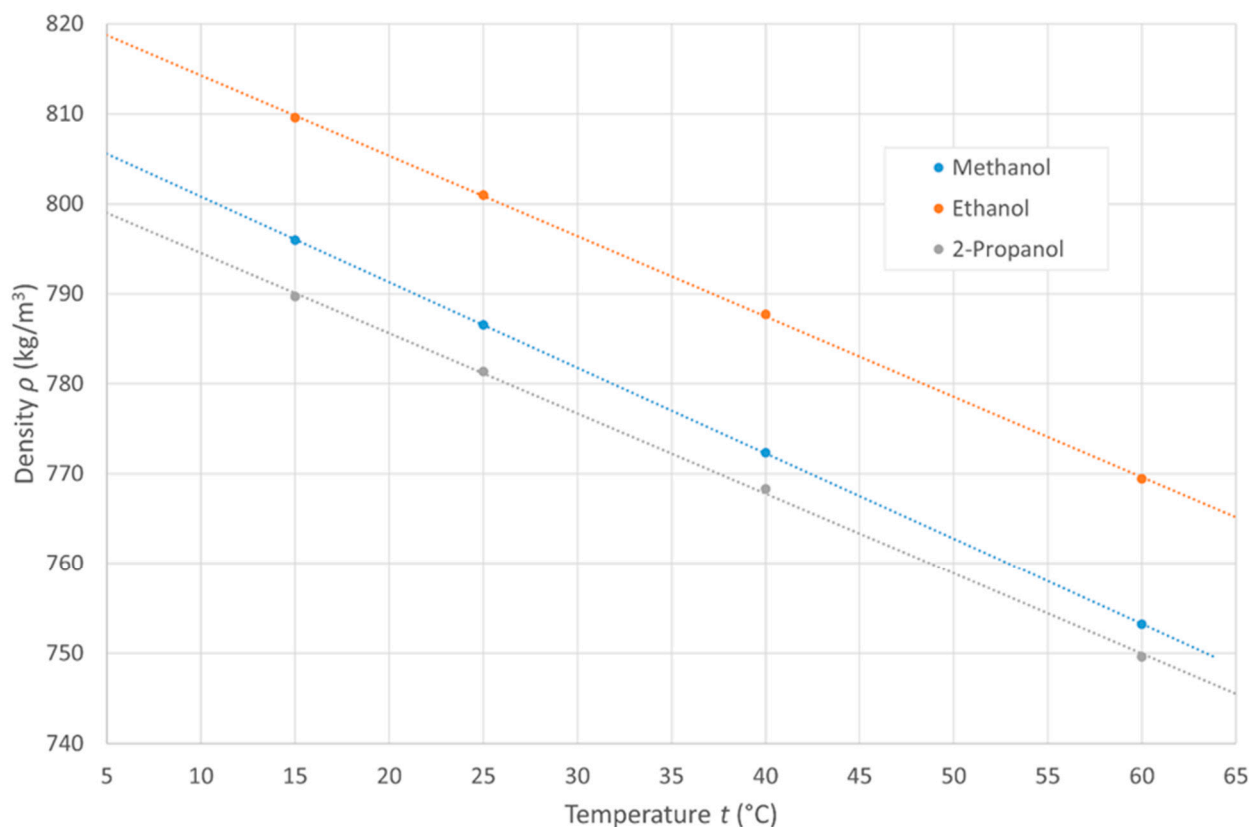$$\varepsilon = \frac{|\rho_{60} - \rho_{15}|}{60 - 15} = \frac{|\rho_{60} - \rho_{15}|}{45}\tag{2}$$

Figure 2. Measured densities of the alcohol fuels under study.

The values of the densities of the tested fuels at a reference temperature of 15 °C, the ε coefficient for the measured densities of the tested alcohols, and the R^2 coefficient of determination that describes the fit of the model (1) to the measured data are shown in Table 5. For all three tested alcohols, the coefficient of determination was $R^2 > 0.999$, so the model has a very good fit with the data.

Table 5. Indicators characterizing the model of temperature change for the density of alcohol fuels under study.

Alcohol	P15 (kg/m^3)	ε (kg/(m$^3 \cdot {}^\circ$C))	R^2 (–)
Methanol	795.96	0.9507	0.9999
Ethanol	809.59	0.9820	0.9998
2-Propanol	789.71	0.8907	0.9994

The kinematic viscosities of the tested fuels are shown in Figure 3. The dotted lines indicate the curves approximating the change in kinematic viscosity as a function of temperature. The highest kinematic viscosity is 2-propanol, and the lowest is methanol. With increasing viscosity, the thickness of the oil film increases, which may translate into less wear for the contacting components separated by a layer of test fluid.

The kinematic viscosity γ_t (mm^2/s) of a liquid is a function of dynamic density and density at a given temperature t (°C), as described by the relationship:

$$\gamma_t = 1000 \frac{\eta_t}{\rho_t}, \tag{3}$$

where η_t (mPa·s) is the dynamic density of the liquid, and 1000 is the conversion factor of the units of measurement.
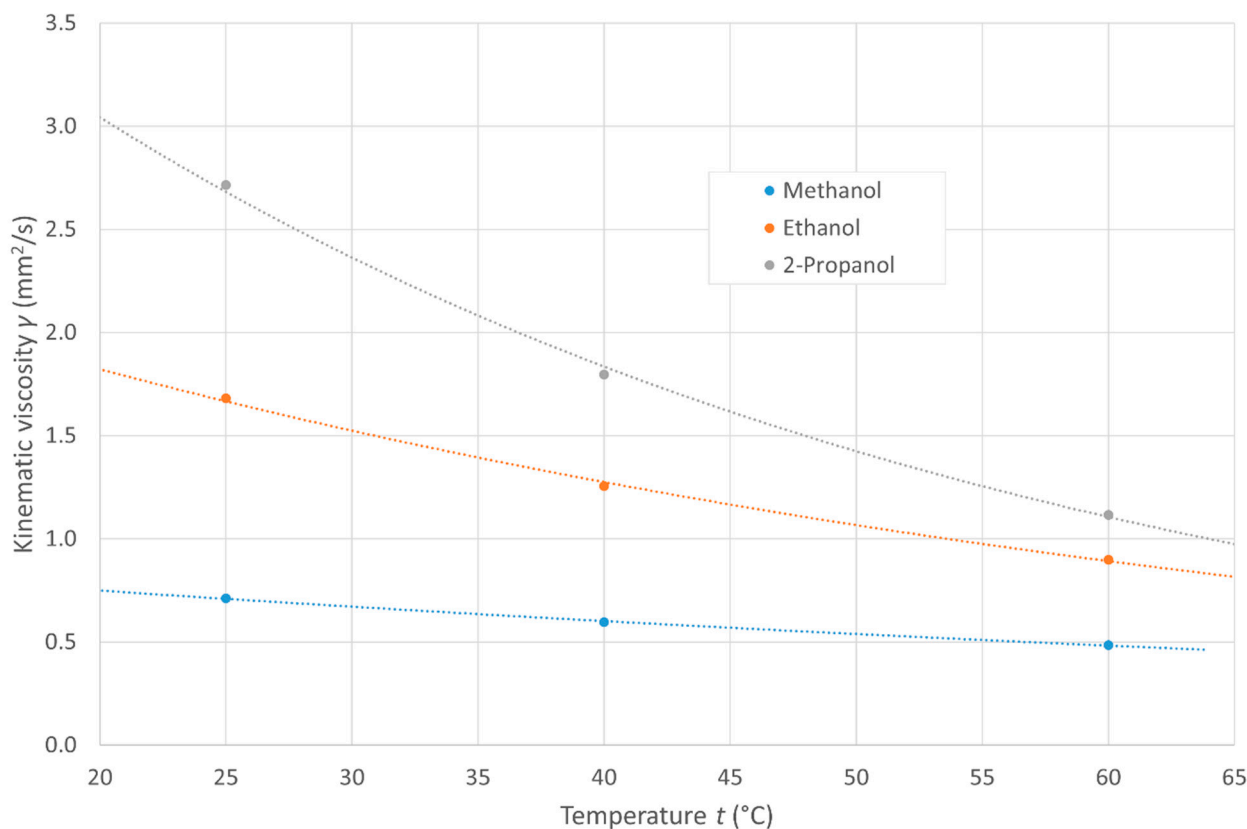
Figure 3. Measured kinematic viscosities of alcohol fuels under study.

The dynamic viscosity of a liquid decreases with increasing temperature according to the exponential Arrhenius–Guzman relationship, i.e.,

$$\eta_t = Ae^{-\frac{\Delta E}{R_C T}},\tag{4}$$

where A is the mass- and molar-volume-dependent characteristic constant for a given liquid, ΔE is the activation energy of viscous flow, R_C involves Clapeyron's gas constant (i.e., $8.31446261815324\ \text{J}\cdot\text{mol}^{-1}\text{K}^{-1}$), and T (K) is the absolute temperature ($T = t + 273.15$).

Taking into account the almost linear dependence of the density of the tested fuels on temperature according to Equation (1), the relationship between kinematic viscosity and temperature, similar to the case of dynamic viscosity, can be approximated by the exponential relation (4) in the form of a function described by the following:
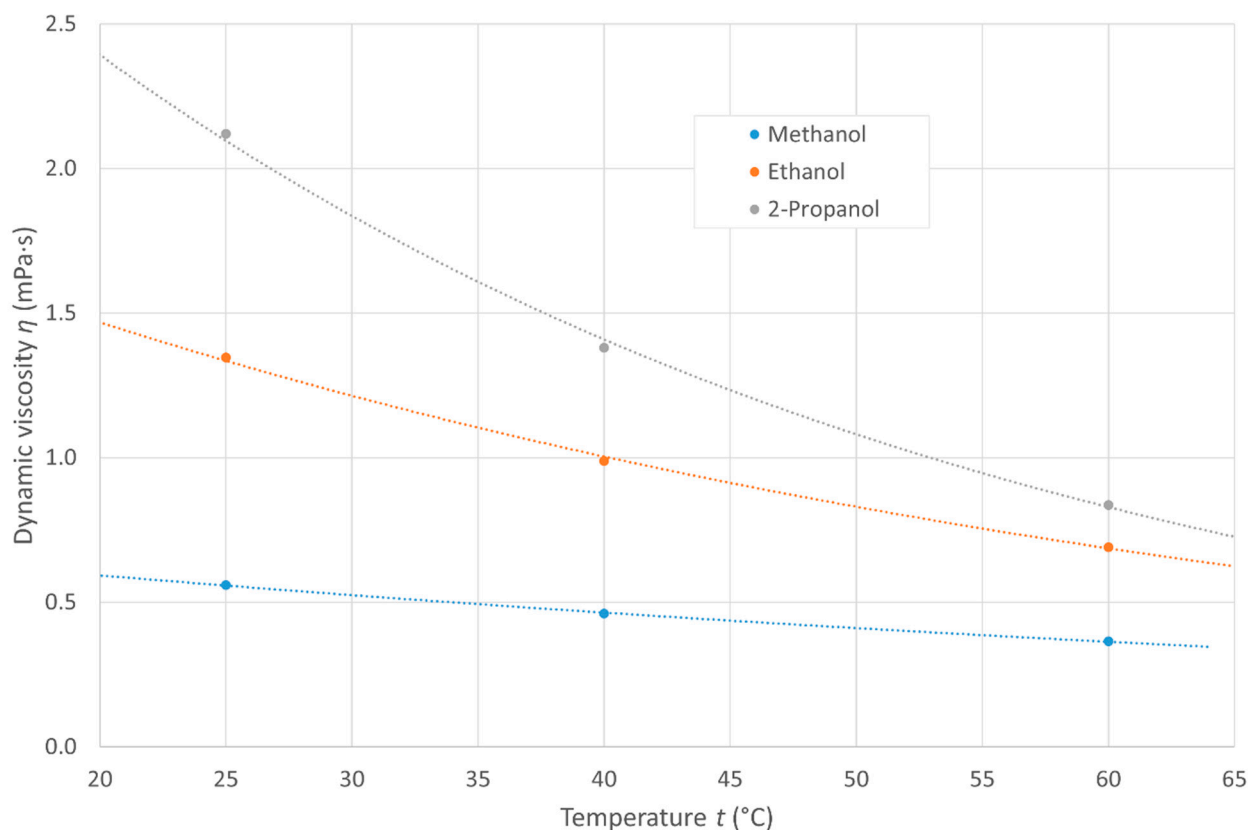
$$\gamma_t = a_1 e^{-a_2 t},\tag{5}$$

where a_1 (mm^2/s) is the scale factor of the temperature model of kinematic viscosity and a_2 ($1/°\text{C}$) is the shape factor of the temperature model of kinematic viscosity.

The values of the coefficients a_1 and a_2 for the measured kinematic viscosities of the tested alcohols, as well as the coefficient of determination R^2, which describes the fit of model (5) to the measured data, are shown in Table 6. For all three tested alcohols, the coefficient of determination was $R^2 > 0.998$, so the model is again a very good fit.

Dynamic viscosity was calculated using the transformed relation (3) for the tested fuels. The values of dynamic viscosity as a function of temperature are shown in Figure 4. The dotted lines indicate the curves approximating each set of measurements.

Table 6. Calculated coefficients of the exponential dependence of kinematic viscosity on the temperature of alcohol fuels under study.

Alcohol	a_1 (mm^2/s)	a_2 (1/°C)	R^2 (–)
Methanol	0.9336	0.011	0.9989
Ethanol	2.6041	0.018	0.9982
2-Propanol	5.0489	0.025	0.9983

Figure 4. Dynamic viscosities of the tested alcohol fuels calculated from measurements.

As an analog to relation (5), according to Equation (3), the dynamic viscosity as a function of temperature can be approximated by an exponential relationship in the form of a function described by the following:

$$\eta_t = b_1 e^{-b_2 t}, \tag{6}$$

where b_1 (mPa·s) is the scale factor of the temperature model of dynamic viscosity and b_2 (1/°C) is the shape factor of the temperature model of dynamic viscosity.

The values of the coefficients b_1 and b_2 for the calculated dynamic viscosities of the tested alcohols, as well as the coefficient of determination R^2 describing the fit of the model (6) to the measured data, are shown in Table 7. For all three tested alcohols, the coefficient of determination was $R^2 > 0.998$; again, the model is a very good fit.

A parameter commonly used to describe the variation of viscosity of petroleum products as a function of temperature is the viscosity index *VI* [46,47]. In the case of the fuels analyzed in the experiment, it is not possible to determine this parameter since it is necessary to know the viscosity of the product at 40 °C and 100 °C in order to determine *VI*; unfortunately, all the tested alcohols have boiling points below 100 °C. To determine the temperature variation of viscosity, the modified viscosity-temperature coefficient (VTC), presented in the literature [48] and determined from previous studies [49], was used and

adapted for present purposes. In the present experiment, the modified coefficient was designated VTC_{25-60} (%) and defined as the relative percentage decrease in kinematic viscosity (mm^2/s) of the tested oil γ_{25} and γ_{60} determined at 25 °C and 60 °C, respectively, relating to the viscosity at 25 °C, as described by the relationship:

$$VTC_{25-60} = 100 \frac{\gamma_{25} - \gamma_{60}}{\gamma_{25}} \tag{7}$$

The largest decrease in viscosity with increasing temperature is shown by 2-propanol and the smallest by methanol. The values of VTC_{25-60} (%) of the tested alcohols are summarized in Table 8.

Table 7. Calculated coefficients of the exponential dependence of dynamic viscosity on the temperature of the alcohol fuels under study.

Alcohol	b_1 (mPa·s)	b_2 (1/°C)	R^2 (–)
Methanol	0.7575	0.012	0.9992
Ethanol	2.1469	0.019	0.9984
2-Propanol	4.0652	0.026	0.9985

Table 8. Temperature change in the kinematic viscosity of the fuels under study.

Parameter	Fuel		
	Methanol	**Ethanol**	**2-Propanol**
VTC_{25-60} (%)	32.02	46.58	58.88

The tested fuels show similar rheological properties and an analogous nature for the changes in individual parameters. Due to the highest viscosity and potentially thickest oil film, the best lubrication conditions will be provided by 2-propanol, followed by ethanol and, finally, methanol.
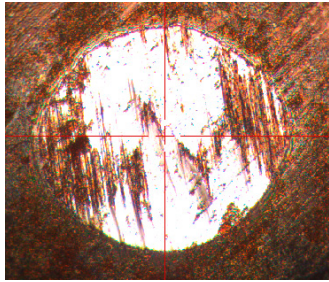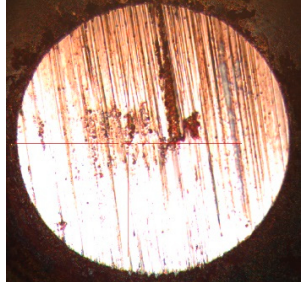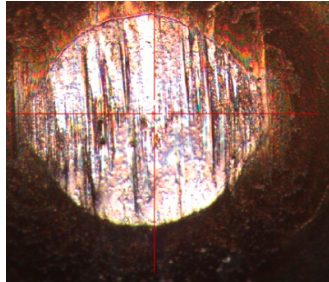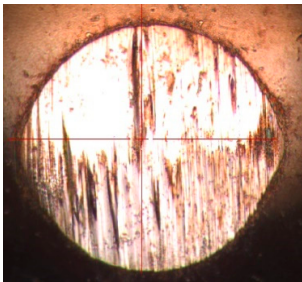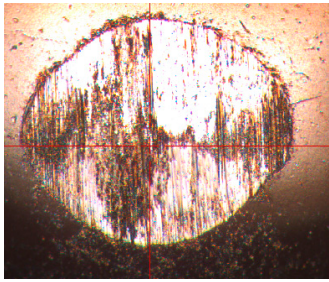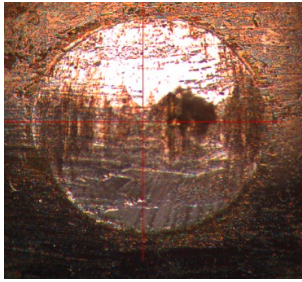
3.2. Lubricity and Auxiliary Indicators

The recorded wear traces of the tested alcohol fuels obtained from HFRR tests at 25 °C for the adopted test execution times are shown in Table 9. All the obtained wear traces are similar in character. The shape of the wear trace is uniform in both directions of the measurement, making it similar to a circle.

The dominant type of wear takes the form of parallel grooves running the entire length of the scar, indicating the dominant influence of plastic deformation. For all tested samples, point-like wear is also evident, which is associated with local micro-cutting, plastic deformation, and scratching of the sample. Thus, for all the tested fuels, the occurrence of analogous phenomena in the wear zone can be assumed.

The corrected magnitude of the wear scar of the tested alcohols is shown in Figure 5. For the standard conditions of the test implementation, according to ASTM D6079-22 at 25 °C and 75 min, the largest wear scar (worst lubricity) was shown by methanol, where the $WS_{1.4}$ value was 736 µm, followed by ethanol with a $WS_{1.4}$ value of 590 µm, and the best lubricity is shown by 2-propanol with a $WS_{1.4}$ value of 489 µm. It should be noted that these values correspond to poor antiwear properties.

Table 9. Recorded wear scars of the sample during the HFRR test of the alcohols under study.

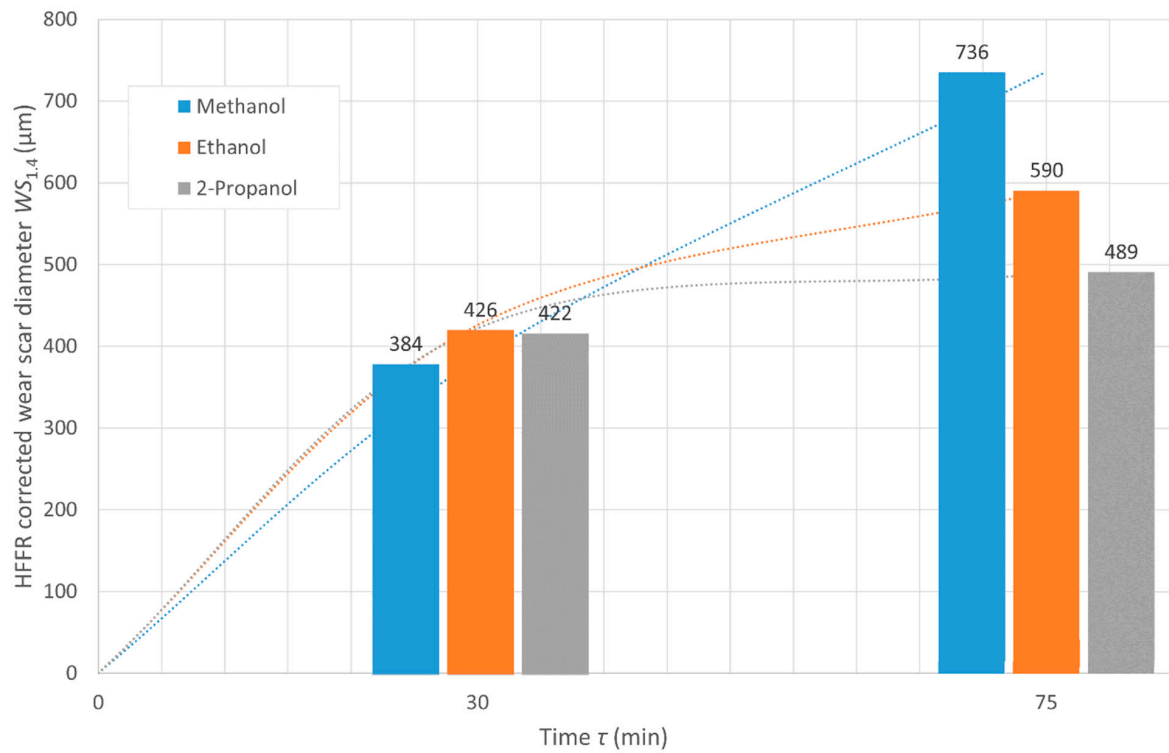| Fuel	Test Execution Time τ = 30 min	Test Execution Time τ = 75 min
Methanol		
Ethanol		
2-Propanol		

Figure 5. Measured values of the corrected average wear scar during the HFRR test of the alcohol fuels under study.

According to the Worldwide Fuel Charter 6th ed. [42] for diesel fuels, the maximum lubricity value of HFRR at 60 °C is 460 μm for fuels cat. 1, 2, and 3 and 400 μm for fuels cat. 4 and 5. According to the EN 590:2022 standard [50], the maximum lubricity value of HFRR at 60 °C is 460 μm. According to the standard for petroleum distillation marine fuels ISO 8217:2024 [51], where the maximum permissible value of $WS_{1.4}$ is 520 μm, which is supposed to ensure adequate durability of precision vapors in the fuel apparatus, only 2-propanol meets analogous requirements. In the case of methanol and ethanol, the value of the corrected wear scar exceeds the normative values, assuming that such values would be obtained at 60 °C. The measurements due to the high volatility of the fuels analyzed were made at the lower temperature of 25 °C, which is indicated in ASTM D6079-24 [40] for fuels of this type. A previous study for diesel fuels shows that the $WS_{1.4}$ values determined for tests at 25 °C are about twice as low as for measurements made at 60 °C [52].

However, the lubricity results obtained are better than the analogous ones obtained using the HFRR test for many additive-free gasoline fuels [53]. For example, European conventional gasoline has $WS_{1.4}$ = 799 μm, CaRFG2 gasoline has $WS_{1.4}$ = 872 μm, CEC RF-83-A-91 gasoline has $WS_{1.4}$ = 711 μm, commercial UK gasoline has $WS_{1.4}$ = 792 μm, and Finland City gasoline has $WS_{1.4}$ = 861 μm [52].

Due to the low lubricity of the tested alcohols, additional measurements were made for the modified standard conditions, i.e., measurement at the standard temperature of 25 °C, but with a shortened measurement time τ of 30 min. In this case, all fuels show a similar $WS_{1.4}$ value, which ranges from 384 μm for methanol through 422 μm for 2-propanol to 426 μm for ethanol. Based on the presented results, it can be concluded that, after a certain measurement duration is exceeded, the wear increases due to a decrease in the amount of the test substance separating the contacting samples due to evaporation caused by friction heating of the samples.

The authors determined the measurement uncertainty values based on the calibration certificates of the measuring instruments used. A summary of the calculated measurement uncertainty values for the analyzed parameters is shown in Table 10. The assessment of measurement uncertainty for secondary and auxiliary quantities was not included in the mentioned table due to their specific nature. The indicated uncertainties refer to normative values.

Table 10. Summary of the uncertainties of the obtained measurement results for each parameter.

Parameter	Symbol	Unit	Methanol	Ethanol	2-Propanol
Density @ 15 °C	$U(\rho 15)$	kg/m^3	0.3509	0.3509	0.3509
Kinematic viscosity @ 40 °C	$U(\nu 40)$	mm^2/s	0.0148	0.0148	0.0148
Lubricity (HFRR wear scar diameter) @ 25 °C	$U(WS_{1.4})$	μm	37.3	37.3	37.3

The average coefficient of friction of the tested fuels during the execution of the test is shown in Figure 6. For a standard HFRR test time τ of 75 min, the highest coefficient of friction equal to 0.369 was obtained for methanol, followed by 0.361 for ethanol, and the lowest value of 0.290 was found for 2-propanol. With a shortened test time τ of 30 min, the highest coefficient of 0.411 was obtained for 2-propanol, next 0.377 for ethanol, and the lowest for methanol at 0.235.
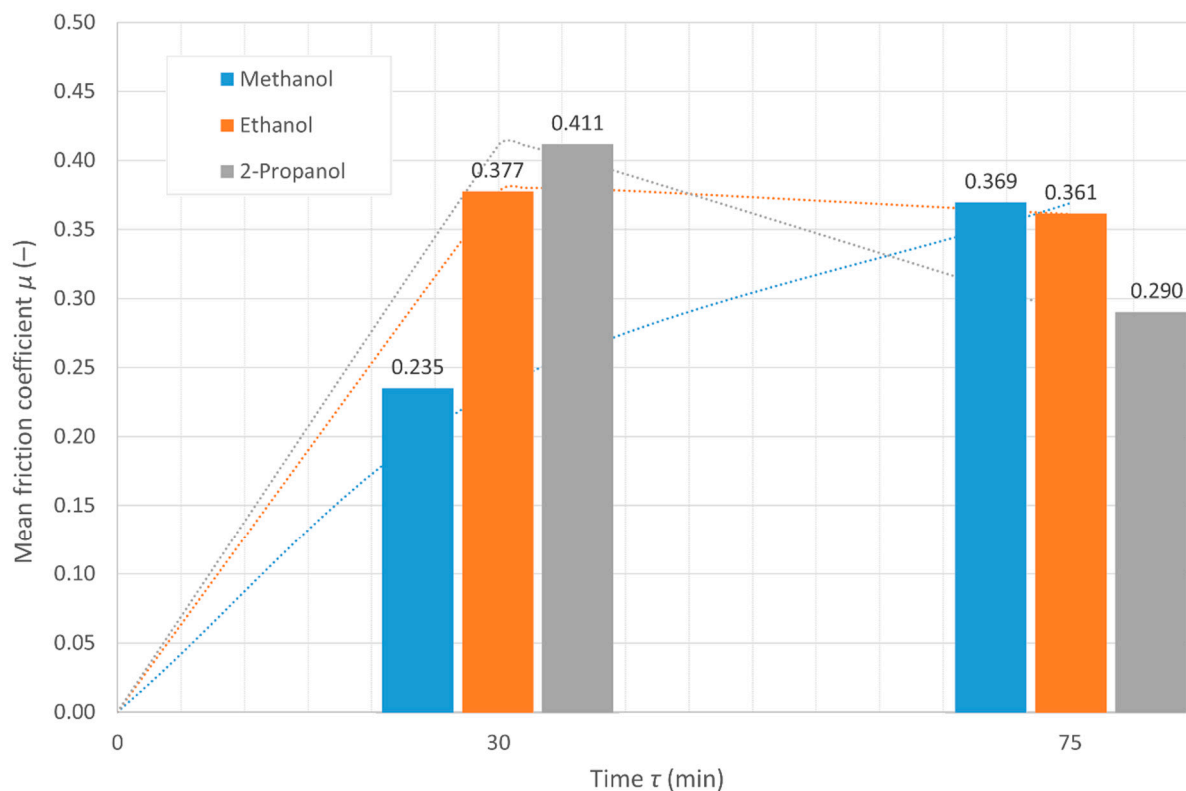
Figure 6. Measured values of the average coefficient of friction during the HFRR test of the alcohol fuels under study.

The average coefficient of friction for the tested alcohols and test execution times is in the range of 0.235–0.411. The values obtained are close to the values of the average coefficient of friction during the HFRR test of gasolines at 25 °C, where the example gasolines obtained a coefficient in the range of 0.320–0.530 [52]. The obtained values of the average coefficient of friction, on the other hand, are much higher than those obtained for diesel fuels, which, at a measurement temperature of 25 °C, are 0.125–0.149, for example, for the distillation fuels for diesel engines [52].

The value of the percentage decrease in oil film *FILM* thickness during the execution of the HFRR test is shown in Figure 7. For both the standard test execution time of 75 min and the test shortened to 30 min, the highest oil *FILM* thickness at the end of the test execution was obtained for methanol, then for 2-propanol, and the highest film thinning was obtained for ethanol. The very low *FILM* parameter values of 24% and 32% for methanol and ≤16% for ethanol and 2-propanol indicate a significant reduction in lubricating *FILM* thickness and periodic metallic contact of the connected samples during the execution of the HFRR test.

The FILM parameter values do not correlate with the viscosity values obtained for individual fuels during previous tests, as shown in Figures 3 and 4, where a lower viscosity is often paired with lower *FILM* parameter values. Such a relationship occurs, for example, for fuel-diluted fresh lubricating oils [54] or fuel-diluted used lubricating oils [55].

In the present experiment for the tested fuels, the mentioned relationship between *FILM* thickness and substance viscosity was not observed, which is presumably due to the fact that the implementation of the HFRR test refers to the evaluation of the ability of individual fuels to form a boundary layer and the analysis of the boundary friction that takes place under these conditions. In contrast, viscosity has a direct effect on the separation of contacting components during the time when the lubricating substance is applied at the appropriate pressure, that is, during hydrostatic or hydrodynamic lubrication. Then, liquid

or mixed friction takes place. An additional factor affecting the obtained results is the low boiling point of the fuels under testing, which results in an accelerated depletion of the amount of the test substance relative to the petroleum-based fuels during the execution of the HFRR test.
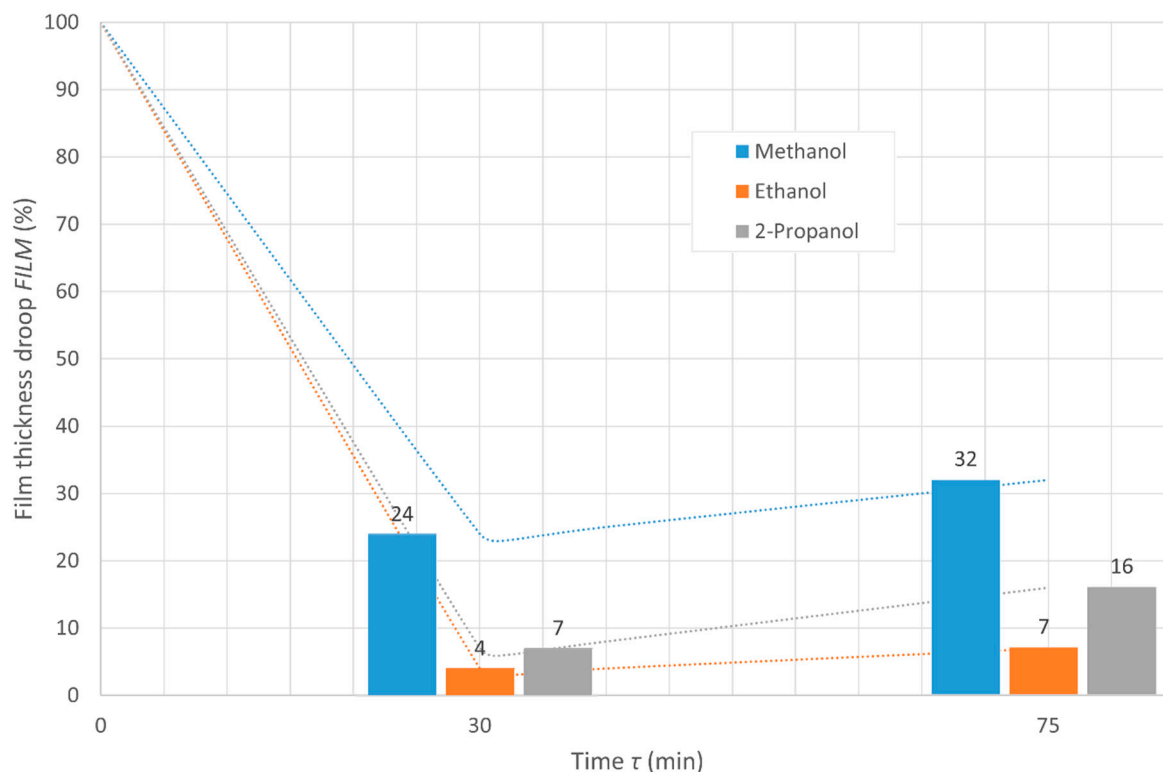

Figure 7. Measured values of thickness drop (resistance) of tested alcohol fuels acting as lubricants during the HFRR test.

4. Conclusions

This study confirmed the low lubricity of the fuels under investigation. Thus, their use in engines may require the use of mixtures of these fuels with hydrocarbons or the application of admixtures to improve the lubricity and, thus, reduce the wear intensity of the components of the tribological pairs lubricated with these fuels.

The lubricity of fuel, and consequently its impact on engine component wear, can be improved by lowering the fuel temperature in the fuel supply system and by using chemical additives that enhance fuel lubricity. Indirectly, the negative impact of fuel on the wear of combustion chamber components, such as cylinder liners, pistons, and piston rings, can be minimized by selecting a lubricating oil that is appropriately matched to the fuel. This approach is analogous to the practice used in industrial and marine engines powered by liquid hydrocarbon fuels with low sulfur content, such as very low sulfur fuels (VLSF) and ultra-low sulfur fuels (ULSF).

The obtained results relating to the rheological characteristics of the studied alcohols can be the basis for further analysis. This is especially true for the developed models of density, kinematic viscosity, and dynamic viscosity, which can be used in subsequent experiments since they provide a very good match between the calculation results and empirical data.

The experiment, as expected, showed that the antiwear properties of alcohols are low. The lubricity is much worse than that of diesel oils, while it is close to that of gasoline. This makes it necessary to use various admixtures to improve the lubricity of pure alcohol fuels and fuels that are mixtures of alcohols, alcohols and gasolines, and alcohols and diesel oils.

The obtained results can be used in further research aimed at optimizing the properties of fuels enriched with bioalcohols or alcohol-based fuels, which is becoming a much more important issue for road users who want to reduce their fossil fuel use. Moreover, the new generation of fuels, in addition to providing adequate ignition and caloric properties, must also exhibit appropriate characteristics to guarantee the reliability, durability, and operational safety of the internal combustion engines that these fuels will power.

Abbreviations

A	characteristic constant for a given liquid
a_1, a_2	coefficients of the equation approximating kinematic viscosity
ASTM	American Society for Testing and Materials
b_1, b_2	coefficients of the equation approximating dynamic viscosity
CN	cetane number
ΔE	activation energy of viscous flow
$FILM$	percentage decrease in film thickness of lubricant during the HFRR test
HFRR	high-frequency reciprocating rig
ISO	International Organization for Standardization
R_C	Clapeyron's gas constant
R^2	coefficient of determination
RON	research octane number
T	absolute temperature expressed in K
t	relative temperature expressed in °C
U	uncertainty
VI	viscosity index
VTC	viscosity-temperature coefficient
VTC_{25-60}	relative percentage decrease in kinematic viscosity with an increase in temperature
$WD_{1.4}$	normalized HFRR wear scar diameter
γ_t	kinematic viscosity at temperature t (°C)
ε	coefficient of temperature change for density
μ	friction coefficient
η_t	dynamic viscosity at temperature t (°C)
ρ	density
ρ_{15}	density at 15 °C
ρ_{60}	density at 60 °C
ρ_t	density at temperature t (°C)
τ	test execution time

Appendix A

Table A1. Measurement data.

Parameter	Temperature (°C)	Time (min)	Unit	Methanol	Ethanol	2-Propanol
Kinematic viscosity	25	N/A	mm^2/s	0.712	1.681	2.714
	40	N/A		0.597	1.256	1.797
	60	N/A		0.484	0.898	1.116
Density	15	N/A	kg/m^3	795.96	809.59	789.71
	25	N/A		786.56	800.96	781.36
	40	N/A		772.33	787.73	768.31
	60	N/A		753.18	769.45	749.63
Water content	N/A	N/A	(% m/m)	0.02	5.50	0.13
Lubricity	25	30	μm	384	426	422
	Coefficient of friction		N/A	0.235	0.377	0.411
	FILM parameter		%	24	4	7
	25	75	μm	736	590	489
	Coefficient of friction		N/A	0.369	0.361	0.290
	FILM parameter		%	32	7	16

Appendix B Empirical Models

Appendix B.1 Density $\rho_t(kg/m^3) = f[t\,(°C)]$

Methanol: $\rho_t = 795.96 - 0.9507(t - 15)$
Ethanol: $\rho_t = 809.59 - 0.9820\,(t - 15)$
2-Propanol: $\rho_t = 789.71 - 0.8907\,(t - 15)$

Appendix B.2 Kinematic Viscosity $\gamma_t(mm^2/s) = f[t\,(°C)]$

Methanol: $\gamma_t = 0.9336e^{-0.011 \cdot t}$
Ethanol: $\gamma_t = 2.6041e^{-0.018 \cdot t}$
2-Propanol: $\gamma_t = 5.0489e^{-0.025 \cdot t}$

Appendix B.3 Dynamic Viscosity $\eta_t(mPa·s) = f[t\,(°C)]$

Methanol: $\eta_t = 0.7575e^{-0.012 \cdot t}$
Ethanol: $\eta_t = 2.1469e^{-0.019 \cdot t}$
2-Propanol: $\eta_t = 4.0652e^{-0.026 \cdot t}$

References

1. Göktaş, M.; Kemal Balki, M.; Sayin, C.; Canakci, M. An Evaluation of the Use of Alcohol Fuels in SI Engines in Terms of Performance, Emission and Combustion Characteristics: A Review. *Fuel* **2021**, *286*, 119425. [CrossRef]
2. Lucke, C.E.; Woodward, S.M. *Tests of Internal-Combustion Engines on Alcohol Fuel*; U.S. Department of Agriculture: Washington, DC, USA, 1907.
3. Taşören, E.; Aydoğan, H.; Gökmen, M.S. Research of Effect on Gasoline-2-Propanol Blends on Exhaust Emission of Gasoline Engine with Direct Enjection Using Taguchi Approach. *Eur. Mech. Sci.* **2021**, *5*, 177–182. [CrossRef]
4. Monique, B. *Vermeire Everything You Need to Know About Marine Fuels*; Chevron Marine Products: Ghent, Belgium, 2021.
5. Herdzik, J. Marine Fuel from the Past to the Future. *Sci. J. Marit. Univ. Szczec. Zesz. Nauk. Akad. Morskiej W Szczecinie* **2023**, *74*, 83–90. [CrossRef]
6. Surisetty, V.R.; Dalai, A.K.; Kozinski, J. Alcohols as Alternative Fuels: An Overview. *Appl. Catal. A Gen.* **2011**. [CrossRef]
7. Calam, A.; Ali, R.; Solmaz, H.; Yücesu, H.S. An Experimental Evaluation of TiO_2 Nanoadditive for HCCI Engines Running on ABE Fuel. *Energy* **2024**, *313*, 133837. [CrossRef]
8. Jamrozik, A.; Tutak, W. Alcohols as Biofuel for a Diesel Engine with Blend Mode—A Review. *Energies* **2024**, *17*, 4516. [CrossRef]

9. Yang, S.; Wan, M.; Shen, L.; Wang, Z.; Huang, F.; Ma, Y.; Xiao, Y. Investigation of the Impacts of Regeneration Temperature and Methanol Substitution Rate on the Active Regeneration of Diesel Particulate Filter in a Diesel-Methanol Dual-Fuel Engine. *Energy* **2024**, *301*, 131657. [CrossRef]

10. Shi, X.; Yu, Z.; Lin, T.; Wu, S.; Fu, Y.; Chen, B. Future Prospects of MeOH and EtOH Blending in Gasoline: A Comparative Study on Fossil, Biomass, and Renewable Energy Sources Considering Economic and Environmental Factors. *Processes* **2024**, *12*, 1751. [CrossRef]

11. Ali Ijaz Malik, M.; Kalam, M.A.; Mujtaba Abbas, M.; Susan Silitonga, A.; Ikram, A. Recent Advancements, Applications, and Technical Challenges in Fuel Additives-Assisted Engine Operations. *Energy Convers. Manag.* **2024**, *313*, 118643. [CrossRef]

12. Zhao, Z.; Liu, P.; Zhao, J.; Huang, H.; Li, X.; Zheng, X.; Liu, Z.; Guo, Q.; Yao, Z.; Zhang, H.; et al. A Photometric-Turbidimetric Fusion Sensor for Measuring the Water Content in Diesel with Sensitivity Increase by the Extended Infrared Path Capillary. *Sens. Actuators B Chem.* **2024**, *412*, 135764. [CrossRef]

13. Duraisamy, B.; Varuvel, E.G.; Palanichamy, S.; Subramanian, B.; Jerome Stanley, M.; Madheswaran, D.K. Impact of Hydrogen Addition on Diesel Engine Performance, Emissions, Combustion, and Vibration Characteristics Using a Prosopis Juliflora Methyl Ester-Decanol Blend as Pilot Fuel. *Int. J. Hydrogen Energy* **2024**, *75*, 12–23. [CrossRef]

14. Mebrahtu, C.; Sun, R.; Gierlich, C.H.; Palkovits, R. Unraveling the Structure-Activity Relationships of Cu/H-BEA Bifunctional Catalyst for Selective Synthesis of Dimethoxymethane by Non-Oxidative Dehydrogenation of Methanol. *Appl. Catal. B* **2021**, *287*, 119964. [CrossRef]

15. EL-Seesy, A.I.; Nour, M.; Hassan, H.; Elfasakhany, A.; He, Z.; Mujtaba, M.A. Diesel-Oxygenated Fuels Ternary Blends with Nano Additives in Compression Ignition Engine: A Step towards Cleaner Combustion and Green Environment. *Case Stud. Therm. Eng.* **2021**, *25*, 100911. [CrossRef]

16. Nour, M.; Sun, Z.; El-Seesy, A.I.; Li, X. Experimental Evaluation of the Performance and Emissions of a Direct-Injection Compression-Ignition Engine Fueled with n-Hexanol–Diesel Blends. *Fuel* **2021**, *302*, 121144. [CrossRef]

17. Chen, H.; Lou, W.; Sun, S.; Wang, X. Analysis of Organic Intermediates with a Low-Load Pd/Al$_2$O$_3$ Catalyst for the Ethanol-SCR of NO at Low Temperatures: The Influential Role of NH3 and Catalyst Characterization. *Fuel* **2021**, *302*, 121101. [CrossRef]

18. Čedík, J.; Pexa, M.; Holúbek, M.; Mrázek, J.; Valera, H.; Agarwal, A.K. Operational Parameters of a Diesel Engine Running on Diesel–Rapeseed Oil–Methanol–Iso-Butanol Blends. *Energies* **2021**, *14*, 6173. [CrossRef]

19. Nashte, A.; SJ, S.P.; Rathod, D. *Investigations of Emission Reduction Potential of Diesel-Methanol Blends in a Heavy-Duty Genset Engine*; FEV India Pvt, Ltd.: Pune, India, 2021.

20. Jing, Z.; Zhang, C.; Cai, P.; Li, Y.; Chen, Z.; Li, S.; Lu, A. Multiple-Objective Optimization of a Methanol/Diesel Reactivity Controlled Compression Ignition Engine Based on Non-Dominated Sorting Genetic Algorithm-II. *Fuel* **2021**, *300*, 120953. [CrossRef]

21. Honeywell Search Chemicals. Available online: https://lab.honeywell.com/ (accessed on 13 July 2024).

22. Stępień, Z. Potencjał Użytkowo-Eksploatacyjny Butanolu Jako Paliwa Alternatywnego Do Zasilania Silników ZI. *Nafta-Gaz.* **2020**, *76*, 126–135. [CrossRef]

23. CIOP PIB Baza Wiedzy o Zagrożeniach Chemicznych i Pyłowych. Available online: https://www.ciop.pl/CIOPPortalWAR/appmanager/ciop/pl?_nfpb=true&_pageLabel=P20200153841377519058042 (accessed on 19 July 2024).

24. Yanowitz, J.; Ratcliff, M.; McCormick, R.; Taylor, J.; Murphy, M. *Compendium of Experimental Cetane Numbers*; National Renewable Energy Laboratory: Golden, CO, USA, 2014.

25. Dierickx, J.; Verbiest, J.; Janvier, T.; Peeters, J.; Sileghem, L.; Verhelst, S. Retrofitting a High-Speed Marine Engine to Dual-Fuel Methanol-Diesel Operation: A Comparison of Multiple and Single Point Methanol Port Injection. *Fuel Commun.* **2021**, *7*, 100010. [CrossRef]

26. Chansauria, P.; Mandloi, R.K. Effects of Ethanol Blends on Performance of Spark Ignition Engine-A Review. *Mater. Today Proc.* **2018**, *5*, 4066–4077. [CrossRef]

27. Wärtsilä Corporation the Wärtsilä 32 Methanol Engine. Available online: https://www.wartsila.com/docs/default-source/product-files/engines/wartsila-32-methanol-leaflet.pdf (accessed on 14 July 2024).

28. InSight Unlocking the Full Potential of Methanol. Available online: https://www.infineuminsight.com/en-gb/articles/unlocking-the-full-potential-of-methanol/ (accessed on 19 July 2024).

29. Gajević, S.; Marković, A.; Milojević, S.; Ašonja, A.; Ivanović, L.; Stojanović, B. Multi-Objective Optimization of Tribological Characteristics for Aluminum Composite Using Taguchi Grey and TOPSIS Approaches. *Lubricants* **2024**, *12*, 171. [CrossRef]

30. Bond, R.E.; Loth, J.L.; Guiler, R.W.; Clark, N.N.; Heydorn, E.C. Lubricity Problems and Solutions for a Methanol Fueled Gas Turbine. In Proceedings of the Rheology and Fluid Mechanics of Nonlinear Materials, Orlando, FL, USA, 5–10 November 2000; American Society of Mechanical Engineers: Houston, TX, USA, 2000; pp. 55–58.

31. Schramm, J. *Alcohol Applications in Compression Ignition Engines*; Technical University of Denmark: Kongens Lyngby, Denmark, 2016.

32. Kuszewski, H.; Jaworski, A.; Ustrzycki, A. Lubricity of Ethanol–Diesel Blends—Study with the HFRR Method. *Fuel* **2017**, *208*, 491–498. [CrossRef]

33.   Kunwer, R.; Ranjit Pasupuleti, S.; Sureshchandra Bhurat, S.; Kumar Gugulothu, S.; Rathore, N. Blending of Ethanol with Gasoline and Diesel Fuel—A Review. *Mater. Today Proc.* **2022**, *69*, 560–563. [CrossRef]

34.   Washecheck, P.H.; Liu, A.T.; Kennedy, E.F. Methanol Fuel and Methanol Fuel Additives. U.S. Patent No. 4,375,360A, 12 January 1981.

35.   Milojević, S.; Glišović, J.; Savić, S.; Bošković, G.; Bukvić, M.; Stojanović, B. Particulate Matter Emission and Air Pollution Reduction by Applying Variable Systems in Tribologically Optimized Diesel Engines for Vehicles in Road Traffic. *Atmosphere* **2024**, *15*, 184. [CrossRef]

36.   *ISO 12185:2024*; Crude Petroleum, Petroleum Products and Related Products—Determination of Density—Laboratory Density Meter with an Oscillating U-Tube Sensor. ISO: Geneva, Switzerland, 2024.

37.   *ISO 3104:2023*; Petroleum Products—Transparent and Opaque Liquids—Determination of Kinematic Viscosity and Calculation of Dynamic Viscosity. SIO: Geneva, Switzerland, 2023.

38.   Malinowska, M.; Zera, D. Analiza Zmian Smarności Oleju Silnikowego Stosowanego w Silniku Cegielski-Sulzer 3AL25/30. *Zesz. Nauk. Akad. Morskiej W Gdyni* **2016**, *96*, 93–104.

39.   *ISO 12156-1:2023*; Diesel Fuel—Assessment of Lubricity Using the High-Frequency Reciprocating Rig (HFRR)—Part 1: Test Method. ISO: Geneva, Switzerland, 2023.

40.   *ASTM D 6079-22*; Standard Test Method for Evaluating Lubricity of Diesel Fuels by the High-Frequency Reciprocating Rig (HFRR). ASTM: West Conshohocken, PA, USA, 2023.

41.   *CEC F-06-96*; Measurement of Diesel Fuel Lubricity (HFRR Fuel Lubricity Tester). CEC Standard: Brussels, Belgium, 1996.

42.   Worldwide Fuel Charter 2019—Gasoline and Diesel Fuel. Available online: https://www.acea.auto/publication/worldwide-fuel-charter-2019-gasoline-and-diesel-fuel/ (accessed on 14 February 2025).

43.   PCS Instruments. *Aparat Do Badania Paliw i Środków Smarnych. Instrukcja Obsługi Systemu HFRR V1.0.3*; Inkom Instruments Co.: Warszawa, Poland, 1999.

44.   PCS Instruments. *Instrukcja Obsługi, Mikroskop Do Pomiaru Skazy Zużycia Na Aparacie HFR2*; Inkom Instruments Co.: Warszawa, Poland, 1999.

45.   Piotrowski, I.; Witkowski, K. *Okrętowe Silniki Spalinowe*, 3rd ed.; Trademar: Gdynia, Poland, 2013; ISBN 978-83-62227-48-8.

46.   Chybowski, L.; Szczepanek, M.; Ćwirko, K.; Marosek, K. Analytical Method for Determining the Viscosity Index of Engine Lubricating Oils. *Energies* **2024**, *17*, 4908. [CrossRef]

47.   *ISO 2909:2002*; Petroleum Products—Calculation of Viscosity Index from Kinematic Viscosity. ISO: Geneva, Switzerland, 2002.

48.   Stanciu, I. Viscosity Index Improvers Dor Multi-Grade Oil of Copolymers Polyethylene-Propylene and Hydrogenated Poly (Isoprene-Co-Styrene). *J. Sci. Arts* **2017**, *4*, 771–778.

49.   Hillman, D.E.; Lindley, H.M.; Paul, J.I.; Pickles, D. Application of Gel Permeation Chromatography to the Study of Shear Degradation of Polymeric Viscosity Index Improvers Used in Automotive Engine Oils. *Br. Polym. J.* **1975**, *7*, 397–407. [CrossRef]

50.   EN 590 Diesel Specifications. Available online: https://www.nationwidefuels.co.uk/fuel-specifications/en-590/ (accessed on 20 December 2024).

51.   *ISO 8217:2024*; Petroleum Products—Fuels (Class. F)—Specifications of Marine Fuels. 7th ed. ISO: Geneva, Switzerland, 2024.

52.   Ping, W.D.; Korcek, S.; Spikes, H. Comparison of the Lubricity of Gasoline and Diesel Fuels. *SAE Trans.* **1996**, *105*, 1650–1658.

53.   Oleksiak, S.; Stępień, Z. Zagadnienia Smarności Paliw Silnikowych. Lubricity of Engine Liquid Fuels. *Czas. Tech. M* **2008**, *7-M/2008*, 251–263.

54.   Chybowski, L.; Kowalak, P.; Dąbrowski, P. Assessment of the Impact of Lubricating Oil Contamination by Biodiesel on Trunk Piston Engine Reliability. *Energies* **2023**, *16*, 5056. [CrossRef]

55.   Chybowski, L.; Szczepanek, M.; Sztangierski, R.; Brożek, P. A Quantitative and Qualitative Analysis of the Lubricity of Used Lubricating Oil Diluted with Diesel Oil. *Appl. Sci.* **2024**, *14*, 4567. [CrossRef]